

KNO scaling in processes of electron-positron annihilation to hadrons

V. A. Abramovsky*, N. V. Radchenko

Novgorod State University, B. S.-Peterburgskaya Street 41,
Novgorod the Great, Russia, 173003

Abstract

The charged particles multiplicity distribution in the KNO form is discussed in processes of e^+e^- annihilation at energies \sqrt{s} 14 – 206.2 GeV. The experimental data are compared to data, obtained with Monte Carlo simulation in PYTHIA in the Lund quark string model. It is shown, that both experimental and simulated data are described by the same distribution function in the KNO form. It is shown, that the KNO scaling is consequence of quark string hadronization dynamics in the Lund string model.

Since the time of publication of Koba, Nielsen and Olesen paper [1] (and also of Polyakov paper [2], which had appeared 2 years earlier) it became clear that the scaling invariance of multiplicity distribution function at high energies, the so-called KNO scaling, gives an important information on character and dynamics of multiple hadron production.

The simplest processes are the processes of hadron production in e^+e^- annihilation, in which hadrons are produced in strings of color field that have quark and antiquark at the endpoints, the so-called quark strings [3].

The advantage of these processes both from theoretic and experimental points of view is that there is no need to take into account the parton distributions in the initial state, unlike in deep inelastic scattering. It allows one to avoid uncertainties connected with the phenomenological character of these parton distributions. Moreover, since there are no hadrons in the initial state, the produced secondary hadrons completely represent the dynamics of quark strings decay (or any other hadronization mechanism).

In the present study we will show that the charged particles multiplicity distribution functions in processes of e^+e^- annihilation to hadrons, obtained experimentally to the total center-of-mass energy 206.2 GeV, satisfy the KNO scaling. We will also show that to this energy contribution to the dynamics of the process is given by the only one quark string, and this is exactly what determines the presence of the KNO scaling.

We consider the process of e^+e^- annihilation at 6 values of total center-of-mass energy – \sqrt{s} from 14 to 206.2 GeV. Wide coverage of the experimental data and sufficient statistical provision of them were criteria for the choice. At the energy 14 GeV the number of events is 2 704 (TASSO) [4], at 29 – 29 649 (HRS) [5], at 34.8 – 52 832

*ava@novsu.ac.ru

(TASSO) [4], at 91.2 – 248 100 (L3) [6], at 188.6 – 4 479 (L3) [6], at 206.2 – 4 146 (L3) [6].

The distribution function $\langle n \rangle P_n$ is shown in Fig.1, where P_n is the probability of production of n charged particles, and $\langle n \rangle$ is the mean multiplicity of the charged particles at given energy. The ordinate axis in Fig.1a is given in linear scale in order to demonstrate coincidence in the main part of the peak. We think that slight discrepancy near the maximum of the distribution is related firstly to the experimental errors, and secondly, but this is the most important in our sight, to transition from the discrete multiplicity distribution to the continuous distribution. Maximum in the discrete distribution is absolutely not required to coincide with true maximum. The behavior of the function in tails of the distribution that correspond to low and high multiplicities is shown in Fig.1b, where the ordinate axis is given in logarithmic scale.

The points at all energies are described by the same distribution function within the errors. In order to more explicitly demonstrate this, the distribution functions $\langle n \rangle P_n$ of the minimal (14 GeV) and the maximal (206.2 GeV) of the discussed here energies are given in Fig.2. Visually all points lie on one curve both for linear scale (Fig.2a) and for logarithmic scale (Fig.2b).

Hence, we can accept that in the energy range from 14 GeV to 206.2 GeV, the distribution function $\langle n \rangle P_n$ has the KNO form

$$\langle n \rangle P_n = \Psi \left(\frac{n}{\langle n \rangle} \right).$$

It results from the KNO scaling that a ratio $\langle n \rangle / D$, where $D = \sqrt{\langle n^2 \rangle - \langle n \rangle^2}$ is a dispersion, does not depend on the energy. These data are given in Table 1. Moreover, the approximate constancy (within the errors) of the experimental values of the highest multiplicity distribution moments, $C_l = \langle n^l \rangle / \langle n \rangle^l$, $l = 3, 4, 5$, also supports the presence of the KNO scaling (Table 2).

The fact of the experimental points lying on the KNO curve in different energy ranges was presented in many papers, in particular, in [4] (\sqrt{s} 3.6 – 43.6 GeV), [5] (\sqrt{s} 14 – 34.5 GeV), [7] (\sqrt{s} 29 – 91.2 GeV), [8] (\sqrt{s} 14 – 91.0 GeV). At the energies higher than 91.2 GeV the curves are not considered, only the ratio $\langle n \rangle / D$ is presented [9] (\sqrt{s} 14 – 200 GeV). In the papers [4], [8], [10] it was emphasized that the KNO scaling in the Lund string model holds only approximate and occurs as the result of an accidental combination of several effects. Particular, it was stated that at low energies energy-momentum conservation law leads to narrowing of the multiplicity distributions. On the other hand, at higher energies production of b quarks and hard gluon emission increase the dispersion of the multiplicity distribution, and together these two effects lead to the appearance of the approximate KNO-scaling.

The results presented in Fig.1 and 2 show good coincidence in so large energy range which, in our opinion, can not be accidental. In what follows we will state the arguments, that the experimentally observed in the energy range from 14 to 206.2 GeV KNO scaling is the consequence of the well defined hadronization dynamics.

All theoretical results, including the first work on the KNO, are obtained in far on energy asymptotic for which the value of $1/\ln \sqrt{s}$ is neglecting small. Moreover, it seems to impossible to get the regularities of such complicated event with many degrees of freedom as multiple hadron production from the first principles of QCD. So we have to use more phenomenological and model approaches. We have chosen the Lund string

model and its realization in Monte Carlo generator PYTHIA [13] that provides good description of lots of the experimental data. It should be noted that PYTHIA does not take into account the KNO scaling phenomenologically [14].

Electron-positron annihilation to hadrons was simulated with PYTHIA at every discussed energy from 14 to 206.2 GeV. The decay process of γ^* (Z^0) was considered without the initial state radiation, values of the other parameters were set by default. There were generated one million events for every energy, and the charged particles multiplicity distributions were analyzed, the obtained results are presented in Fig.3.

The distribution function $\langle n \rangle P_n$ has the KNO form at every energy. The simulated values of mean multiplicity $\langle n \rangle$, dispersion D and ratio $\langle n \rangle / D$ are presented in Table 1. All these values are in good agreement with the experimental data. The values of moments C_3, C_4, C_5 are presented in Table 2, they are also coincide with the experimental values. If one combines Fig.1 and Fig.3 then we get good visual agreement of the experimental and simulated data. In what follows we will consider that both distributions are described by the same KNO function.

It was noted before that the main process of hadronization in e^+e^- annihilation is decay of quark string of color field. This string appears between flying quark-antiquark pair produced from γ^* or Z^0 . The mean number of hadrons produced from decay of the quark string is associated with the string length in rapidity space, l . We will not concretize this dependence here. The quark-antiquark pair produced from γ^* (Z^0) can produce the bremsstrahlung gluons which in their turn can produce additional quark-antiquark pairs. The other bremsstrahlung gluons are assimilated by the quark-antiquark pairs producing in the string decay process. Therefore, besides one quark string, there can be several strings, each of which will pass into hadrons.

The distributions of number of strings obtained from the same PYTHIA simulated events for every energy are presented in Table 3. As the string length in rapidity space we take the value

$$l = \ln \frac{(P_i + P_j)^2}{(m_i + m_j)^2},$$

where P_i, P_j are the four-momentum of the quarks that hold the string endpoints, m_i, m_j are the constituent masses of these quarks. The mean summarized string length, the mean charged particles multiplicity and the weight of the corresponding events for events with one string, two strings and so on are presented.

One can imagine the following hadronization picture in e^+e^- hadronization. At the low energies there is only one quark string between quark-antiquark pair produced from γ^* (Z^0) (Fig.4a). Production of an additional pair is suppressed, its probability is only few percents. With the growing energy the weight of the additional quark-antiquark pair is increasing. This pair can lead to splitting of one quark string to two strings (Fig.4b). Since the additional quark and antiquark have approximately the same momenta the endpoints of string from this pair will not be far from each other in rapidity space. So we can consider these two strings as one string without splitting and with the effective length equal to the sum of the lengths of two strings.

As it is seen from Table 3, the lengths of one and two strings for every energy are fully placed in the allowed rapidity phase space, which is defined as $\ln[s/4(m_{ud})^2]$, where $m_{ud} = 0.33$ GeV is the constituent mass of u and d quarks. For the energies under consideration it gives 6.10; 7.56; 7.93; 9.86; 11.30 and 11.50 accordingly. The smaller length of one quark string is bound with the radiation of several bremsstrahlung

gluons by the quark-antiquark pair produced from $\gamma^* (Z^0)$, thus decreasing the energies of quark and antiquark. The precise KNO scaling by its definition must not depend on the energy of flying quarks, i.e. it must not depend on the string length. Therefore, both for one and two quark strings the KNO distribution function $\Psi(n/ \langle n \rangle)$ will have the same form; resulting function will present the sum of these two identical distributions. Violation of the KNO appears only when strings overlap, as it was shown in [15]. But overlapping of the strings is possible only when two or more additional quark-antiquark pairs appear, i.e. when there are three or more quark strings (Fig.4c). The summarized weight of these processes is only 3% at 206.2 GeV (Table 3). Therefore the KNO scaling is not violated for all energies considered in this paper. In order to check the assumption of equivalence of two quark strings to one effective string, the charged particle multiplicity distribution functions in the KNO form were obtained separately for events with only one quark string and for events with two quark strings. The KNO distribution function for events with one string is shown in Fig.5 (the ordinate axis is given in linear scale). The multiplicity distribution for events with two quark strings practically entirely coincides with the case of one string. At that time the KNO scaling is strongly violated when one draws the charged particles distribution function in the KNO form for events with three quark strings.

If one combines the distributions $\Psi(n/ \langle n \rangle)$ given in Fig.1a, Fig.3a and Fig.5, which are drawn in the same scale, then we obtain the completely coincidence of all distributions.

Hence, we can state that the KNO scaling obtained for all experimental data at the energy range 14 – 206.2 GeV is not accidental. We have based on the Lund string model of quark string which, as one can expect, describes the main characteristics of the multiple hadron production well.

Authors are grateful for A. V. Dmitriev and N. V. Prikhod'ko for useful discussions.

This work was partially supported by RFBR grant 07-07-96410-r center-a.

References

- [1] Z. Koba, H. B. Nielsen, P. Olesen, Nucl. Phys. **B40**, 317 (1972).
- [2] A. M. Polyakov, ZhETF **59**, 542 (1970).
- [3] J. Kogut, L. Suskird, Phys. Rev. **D10**, 732 (1974).
S. Brodsky, J. Gunion, Phys. Rev. Lett. **37**, 402 (1976).
E. G. Gurvich, Phys. Lett. **87B**, 386 (1979).
A. Casher, H. Neuberger, S. Nussinov, Phys. Rev. **D20**, 179 (1979).
- [4] W. Braunschweig, R. Gerhards, F.J. Kirschfink et al., Z. Phys. **C45**, (1989).
- [5] M. Derrick, K. K. Gan, P. Kooijman et al., Phys. Rev. **D34**, 3304 (1986).
- [6] P. Achard, O. Adriani, M. Aguilar-Benitez et al., CERN-PH-EP/2004-024 (2004).
- [7] P. D. Acton, G. Alexander, J. Allison et al., Z. Phys. **C53**, 539 (1992).
- [8] P. Abreu, W. Adam, F. Adami et al., Z. Phys. **C50**, 185 (1991).

- [9] P. Abreu, W. Adam, T. Adye et al., Eur. Phys. J. **C18**, 203 (2000).
- [10] M. G. Bowler, P. N. Burrows, Z. Phys. **C31**, 327 (1986).
- [11] B. Andersson, G. Gustafson, G. Ingelman, T. Sjostrand, Phys. Rep. **97**, 31 (1983).
- [12] T. Sjostrand, Phys. Lett. **142B**, 420 (1984).
Nucl. Phys. **B248**, 469 (1984).
- [13] T. Sjostrand, S. Mrenna and P. Skands, JHEP05 (2006) 026 (LU TP 06-13, FERMILAB-PUB-06-052-CD-T) [hep-ph/0603175].
- [14] T. Sjostrand, FERMILAB-Pub-85/119-T (1985).
- [15] V. A. Abramovsky, O. V. Kancheli, Pis'ma v ZhETF, **31**, 566 (1980).

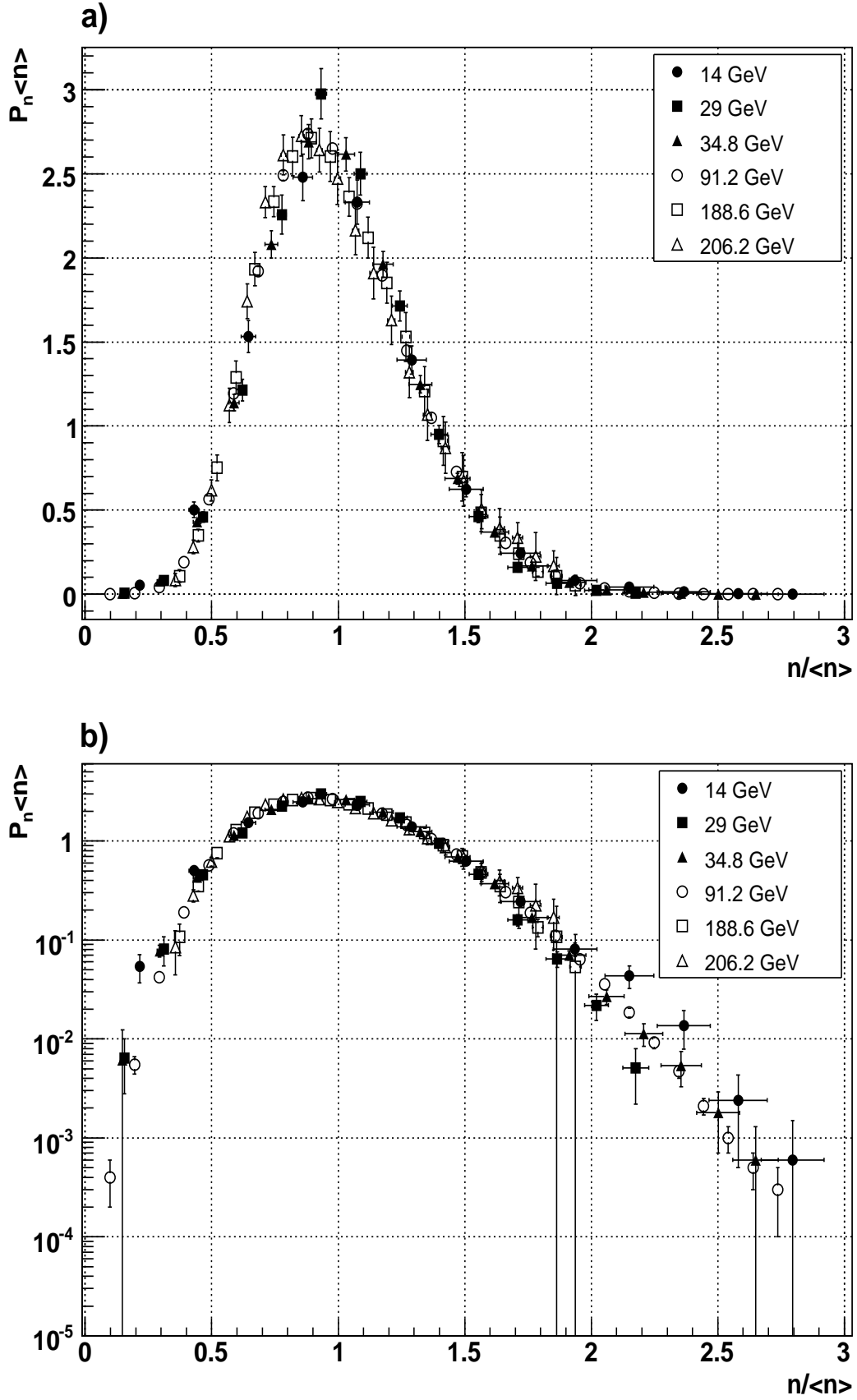


Fig.1. The experimental KNO distribution. Both static and systematic errors are included

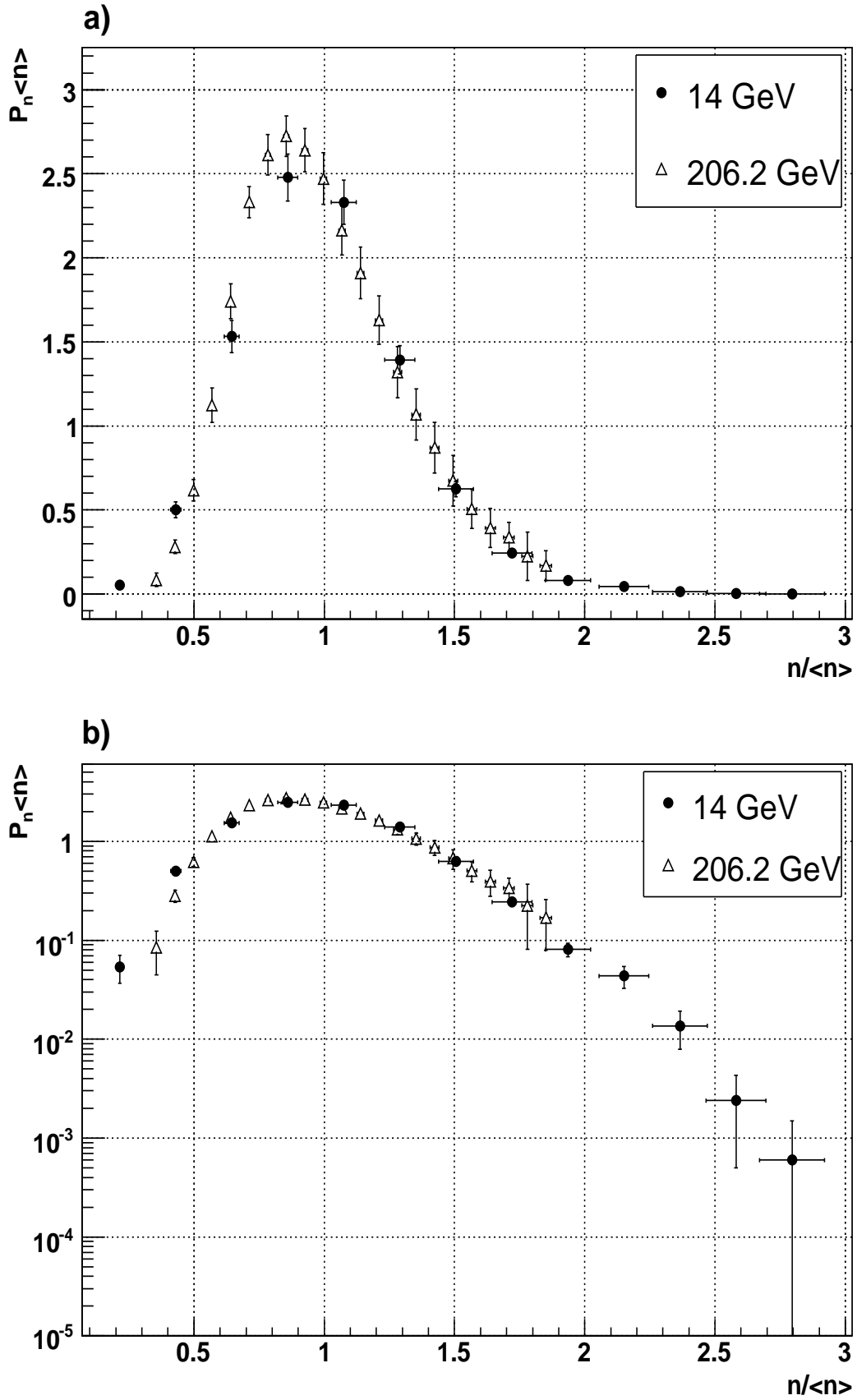


Fig.2. The experimental KNO distribution. Both static and systematic errors are included

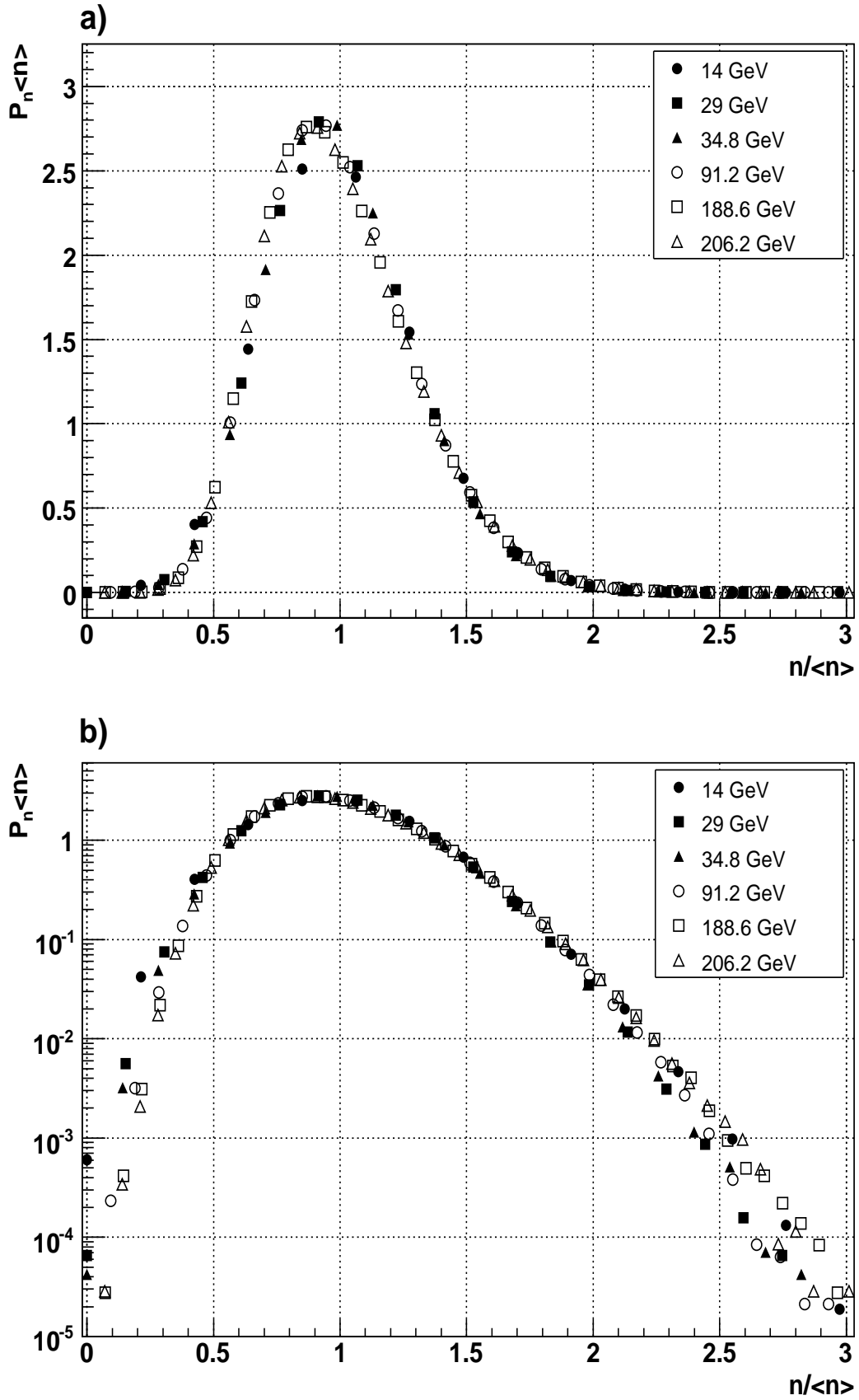


Fig.3. KNO distribution generated by PYTHIA

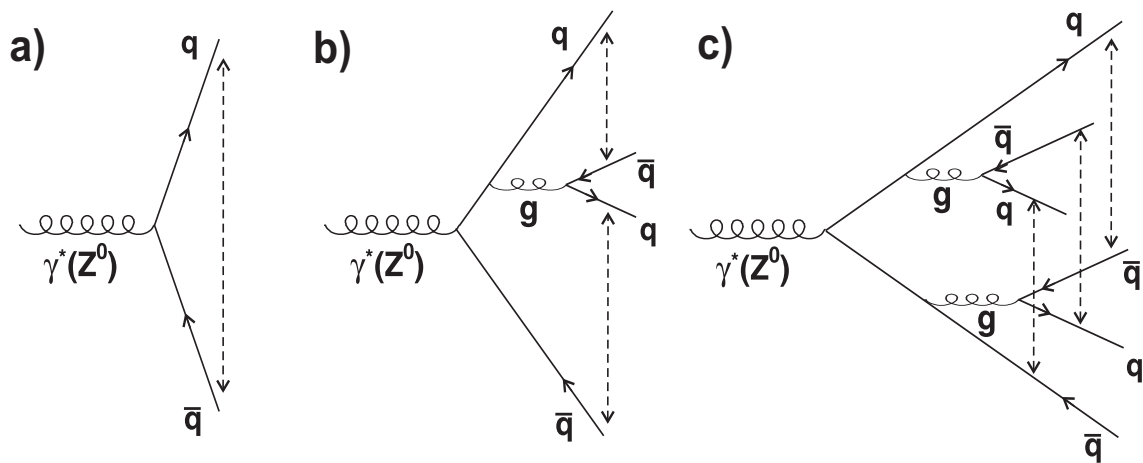


Fig.4.

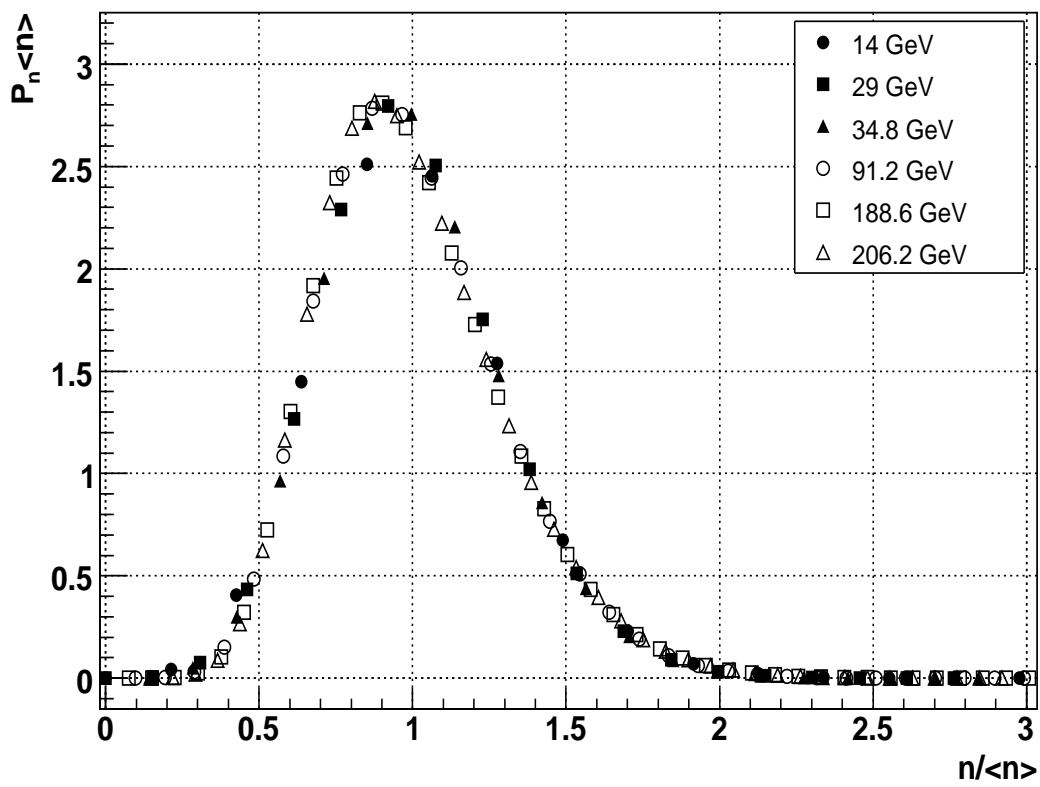


Fig.5. The KNO distribution generated in PYTHIA for events with on quark string

Table 1.

Experimental data			
\sqrt{s} , GeV	$\langle n \rangle$	D	$\langle n \rangle / D$
14	9.30 ± 0.41	3.07 ± 0.28	3.03 ± 0.31
29	12.87 ± 0.30	3.67 ± 0.18	3.51 ± 0.18
34.8	13.59 ± 0.05	4.14 ± 0.39	3.28 ± 0.33
91.2	20.46 ± 0.11	6.24 ± 0.08	3.28 ± 0.05
188.6	26.84 ± 0.32	7.89 ± 0.22	3.40 ± 0.10
206.2	28.09 ± 0.33	8.43 ± 0.22	3.33 ± 0.10
Data generated by PYTHIA			
14	9.41	2.92	3.23
29	13.11	3.84	3.41
34.8	14.17	4.14	3.43
91.2	21.16	6.28	3.37
188.6	27.65	8.35	3.31
206.2	28.56	8.65	3.30

Table 2.

\sqrt{s} , GeV	C_3	C_4	C_5
Experimental data			
14	1.35 ± 0.08	1.78 ± 0.14	2.56 ± 0.24
29	1.25 ± 0.06	1.54 ± 0.08	2.00 ± 0.12
34.8	1.29 ± 0.05	1.64 ± 0.08	2.23 ± 0.14
91.2	1.30 ± 0.01	1.66 ± 0.02	2.27 ± 0.03
188.6	1.26 ± 0.06	1.58 ± 0.09	2.08 ± 0.16
206.2	1.26 ± 0.06	1.58 ± 0.09	2.11 ± 0.16
Data generated by PYTHIA			
14	1.30	1.66	2.25
29	1.27	1.58	2.10
34.8	1.27	1.58	2.09
91.2	1.28	1.61	2.17
188.6	1.29	1.65	2.26
206.2	1.29	1.65	2.26

Table 3.

	Number of strings			
	1	2	3	4
$\sqrt{s} = 14$				
String length, l	3.75	5.52		
$\langle n \rangle$	9.41	10.10		
Weight of event, %	98.59	1.41		
$\sqrt{s} = 29$				
String length, l	4.83	6.70	8.99	
$\langle n \rangle$	13.03	14.62	15.81	
Weight of event, %	95.24	4.70	0.06	
$\sqrt{s} = 34.8$				
String length, l	5.21	7.05	9.29	
$\langle n \rangle$	14.06	15.84	17.34	
Weight of event, %	94.08	5.81	0.11	
$\sqrt{s} = 91.2$				
String length, l	6.66	8.87	11.59	14.02
$\langle n \rangle$	20.72	23.66	26.57	28.95
Weight of event, %	85.83	13.27	0.87	0.03
$\sqrt{s} = 188.6$				
String length, l	8.09	10.63	13.64	16.55
$\langle n \rangle$	26.59	30.67	34.84	38.58
Weight of event, %	76.97	20.38	2.46	0.19
$\sqrt{s} = 206.2$				
String length, l	8.24	10.85	13.89	17.04
$\langle n \rangle$	27.40	31.61	35.80	39.81
Weight of event, %	75.75	21.23	2.80	0.23